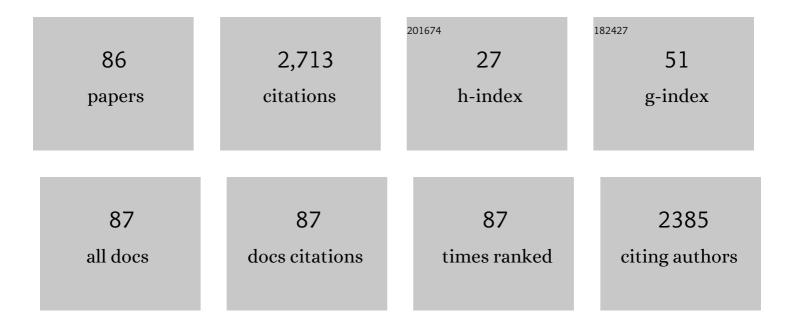
Michael H Frosz

List of Publications by Year in descending order

Source: https://exaly.com/author-pdf/6633759/publications.pdf Version: 2024-02-01



MICHAEL H EDOSZ

#	Article	IF	CITATIONS
1	Efficient Excitation of High-Purity Modes in Arbitrary Waveguide Geometries. Journal of Lightwave Technology, 2022, 40, 1150-1160.	4.6	3
2	Stimulated Brillouin scattering in chiral photonic crystal fiber. Photonics Research, 2022, 10, 711.	7.0	19
3	Hollow-core optical fibre sensors for operando Raman spectroscopy investigation of Li-ion battery liquid electrolytes. Nature Communications, 2022, 13, 1651.	12.8	61
4	Seven-octave high-brightness and carrier-envelope-phase-stable light source. Nature Photonics, 2021, 15, 277-280.	31.4	57
5	Optofluidic Photonic Crystal Fiber Microreactors for In Situ Studies of Carbon Nanodot-Driven Photoreduction. Analytical Chemistry, 2021, 93, 895-901.	6.5	13
6	Cross-phase modulational instability of circularly polarized helical Bloch modes carrying optical vortices in a chiral three-core photonic crystal fiber. Optics Letters, 2021, 46, 174.	3.3	5
7	Optical Fibers: Materials and Applications. Optical Materials Express, 2021, 11, 1364.	3.0	0
8	Optical Fibers: Materials and Applications. Optical Materials Express, 2021, 11, 1364.	3.0	0
9	Scaling rules for high quality soliton self-compression in hollow-core fibers. Optics Express, 2021, 29, 19147.	3.4	23
10	Importance of Topological Charge Preservation in Vectorial Modulational Instability in Chiral Three-Core PCF. , 2021, , .		0
11	Seven-octave Ultra-bright Pulse Generation. , 2021, , .		1
12	Efficient Holographic Excitation of Modes in Hollow-Core Photonic Crystal Fibre. , 2021, , .		0
13	340 - 40,000 nm coherent light source. , 2021, , .		0
14	Three-photon head-mounted microscope for imaging deep cortical layers in freely moving rats. Nature Methods, 2020, 17, 509-513.	19.0	88
15	Progress toward third-order parametric down-conversion in optical fibers. Physical Review A, 2020, 101, .	2.5	15
16	Bragg reflection and conversion between helical Bloch modes in chiral three-core photonic crystal fiber. Journal of Lightwave Technology, 2020, , 1-1.	4.6	4
17	In-Situ Raman Spectroscopy of Reaction Products in Optofluidic Hollow-Core Fiber Microreactors l'? 17. , 2020, , .		2
18	Robust excitation and Raman conversion of guided vortices in a chiral gas-filled photonic crystal fiber. Optics Letters, 2020, 45, 1766.	3.3	7

#	Article	IF	CITATIONS
19	Cross-phase Modulational Instability of Vortex Modes in a Twisted Three-Core Photonic Crystal Fibre. , 2020, , .		1
20	Supercontinuum Generation with Circularly Polarized Vortex Modes in a Chiral Three-Core PCF. , 2020, , .		1
21	Photoreduction in Optofluidic Hollow-Core Photonic Crystal Fiber. , 2019, , .		0
22	Fabrication and Characterization of Tapered Single-Ring Hollow-Core Photonic Crystal Fibre. , 2019, , .		1
23	MRI-guided robotic arm drives optogenetic fMRI with concurrent Ca2+ recording. Nature Communications, 2019, 10, 2536.	12.8	24
24	Fabrication and non-destructive characterization of tapered single-ring hollow-core photonic crystal fiber. APL Photonics, 2019, 4, .	5.7	24
25	Polarization-Tailored Raman Frequency Conversion in Chiral Gas-Filled Hollow-Core Photonic Crystal Fibers. Physical Review Letters, 2019, 122, 143902.	7.8	8
26	Non-Invasive Real-Time Characterization of Hollow-Core Photonic Crystal Fibres using Whispering Gallery Mode Spectroscopy. , 2019, , .		1
27	Spatio-temporal measurement of ionization-induced modal index changes in gas-filled PCF by prism-assisted side-coupling. Optics Express, 2019, 27, 14392.	3.4	6
28	Non-invasive real-time characterization of hollow-core photonic crystal fibers using whispering gallery mode spectroscopy. Optics Express, 2019, 27, 30842.	3.4	9
29	Pump-probe multi-species CARS in a hollow-core PCF with a 20  ppm detection limit under ambient conditions. Optics Letters, 2019, 44, 2486.	3.3	4
30	Generation of broadband circularly polarized supercontinuum light in twisted photonic crystal fibers. Optics Letters, 2019, 44, 3964.	3.3	17
31	Full-field characterization of helical Bloch modes guided in twisted coreless photonic crystal fiber. Optics Letters, 2019, 44, 5049.	3.3	7
32	Spatio-temporal Measurement of Ionization-induced Modal Index Evolution in Gas-filled Hollow-core Photonic Crystal Fiber. , 2019, , .		0
33	Excitation of higher-order modes in optofluidic hollow-core photonic crystal fiber. , 2018, , .		1
34	Excitation of higher-order modes in optofluidic photonic crystal fiber. Optics Express, 2018, 26, 30245.	3.4	15
35	Strong circular dichroism for the HE ₁₁ mode in twisted single-ring hollow-core photonic crystal fiber. Optica, 2018, 5, 1315.	9.3	42
36	Broadband multi-species CARS in gas-filled hollow-core photonic crystal fiber. , 2018, , .		0

Broadband multi-species CARS in gas-filled hollow-core photonic crystal fiber. , 2018, , . 36

3

#	Article	IF	CITATIONS
37	High average power and single-cycle pulses from a mid-IR optical parametric chirped pulse amplifier. Optica, 2017, 4, 1024.	9.3	165
38	Generation of broadband mid-IR and UV light in gas-filled single-ring hollow-core PCF. Optics Express, 2017, 25, 7637.	3.4	65
39	Analytical formulation for the bend loss in single-ring hollow-core photonic crystal fibers. Photonics Research, 2017, 5, 88.	7.0	64
40	Low-loss anti-resonant hollow fibers with polygonal cores. , 2017, , .		0
41	Higher-order mode suppression in twisted single-ring hollow-core photonic crystal fibers. Optics Letters, 2017, 42, 2074.	3.3	29
42	Continuously wavelength-tunable high harmonic generation via soliton dynamics. Optics Letters, 2017, 42, 1768.	3.3	17
43	Single-cycle, 9.6-W, mid-IR pulses via soliton selfcompression from a 21-W OPCPA at 3.25 μm and 160 kHz. , 2017, , .		0
44	Supercontinuum generation in ZBLAN glass photonic crystal fiber with six nanobore cores. Optics Letters, 2016, 41, 4245.	3.3	36
45	Current sensing using circularly birefringent twisted solid-core photonic crystal fiber. Optics Letters, 2016, 41, 1672.	3.3	33
46	Broadband robustly single-mode hollow-core PCF by resonant filtering of higher-order modes. Optics Letters, 2016, 41, 1961.	3.3	222
47	Reducing losses in solid-core photonic crystal fibers using chlorine dehydration. Optical Materials Express, 2016, 6, 2975.	3.0	3
48	Twist-induced guidance in coreless photonic crystal fiber: A helical channel for light. Science Advances, 2016, 2, e1601421.	10.3	62
49	High-resolution wavefront shaping with a photonic crystal fiber for multimode fiber imaging. Optics Letters, 2016, 41, 497.	3.3	51
50	Twist-Tuning of Higher-Order Mode Suppression in Single-Ring Hollow-Core Photonic Crystal Fibers. , 2016, , .		3
51	Enhanced optical activity and circular dichroism in twisted photonic crystal fiber. Optics Letters, 2015, 40, 4639.	3.3	25
52	Compressing μJ-level pulses from 250  fs to sub-10  fs at 38-MHz repetition rate using two ga hollow-core photonic crystal fiber stages. Optics Letters, 2015, 40, 1238.	as-filled	64
53	Damage-free single-mode transmission of deep-UV light in hollow-core PCF. Optics Express, 2014, 22, 15388.	3.4	49
54	Real-time Doppler-assisted tomography of microstructured fibers by side-scattering. Optics Express, 2014, 22, 25570.	3.4	10

#	Article	IF	CITATIONS
55	Orbital-angular-momentum-preserving helical Bloch modes in twisted photonic crystal fiber. Optica, 2014, 1, 165.	9.3	133
56	Doppler-Assisted Tomography of Photonic Crystal Fiber Structure by Side-Scattering. , 2014, , .		0
57	Five-ring hollow-core photonic crystal fiber with 18ÂdB/km loss. Optics Letters, 2013, 38, 2215.	3.3	23
58	Kagome hollow-core photonic crystal fiber probe for Raman spectroscopy. Optics Letters, 2012, 37, 4371.	3.3	58
59	Nonlinear fiber-optic strain sensor based on four-wave mixing in microstructured optical fiber. Optics Letters, 2012, 37, 794.	3.3	46
60	Highly sensitive and simple method for refractive index sensing of liquids in microstructured optical fibers using four-wave mixing. Optics Express, 2011, 19, 10471.	3.4	68
61	Validation of input-noise model for simulations of supercontinuum generation and rogue waves. Optics Express, 2010, 18, 14778.	3.4	119
62	Validation of Input-noise Model for Simulations of Supercontinuum Generation and Rogue Waves. , 2010, , .		0
63	Dispersion-modulation by high material loss in microstructured polymer optical fibers. Optics Express, 2009, 17, 17950.	3.4	3
64	Dispersion-engineered and highly nonlinear microstructured polymer optical fibres. Proceedings of SPIE, 2009, , .	0.8	2
65	Broadband light generation at ~1300 nm through spectrally recoiled solitons and dispersive waves. Optics Letters, 2008, 33, 621.	3.3	20
66	Back-seeding of higher order gain processes in picosecond supercontinuum generation. Optics Express, 2008, 16, 11954.	3.4	53
67	Increasing the blue-shift of a supercontinuum by modifying the fiber glass composition. Optics Express, 2008, 16, 21076.	3.4	28
68	Picosecond supercontinuum generation with back seeding of different spectral parts. , 2008, , .		0
69	Back seeding of picosecond supercontinuum generation in photonic crystal fibres. Proceedings of SPIE, 2008, , .	0.8	Ο
70	Supercontinuum generation in photonic crystal fibers using quasi-CW pumping. , 2007, , .		0
71	The role of the second zero-dispersion wavelength in generation of supercontinua and bright-bright soliton-pairs across the zero-dispersion wavelength: erratum. Optics Express, 2007, 15, 5262.	3.4	3
72	Can pulse broadening be stopped?. Nature Photonics, 2007, 1, 611-612.	31.4	6

#	Article	IF	CITATIONS
73	Nanoengineering of photonic crystal fibers for supercontinuum spectral shaping. Journal of the Optical Society of America B: Optical Physics, 2006, 23, 1692.	2.1	46
74	Soliton collision and Raman gain regimes in continuous-wave pumped supercontinuum generation. Optics Express, 2006, 14, 9391.	3.4	120
75	Extraction of tissue optical properties from optical coherence tomography images for diagnostic purposes (Invited Paper). , 2005, , .		9
76	Supercontinuum generation in a photonic crystal fiber tapered to normal dispersion for all wavelengths. , 2005, , .		0
77	Nano-engineering of photonic crystal fibers for supercontinuum generation. , 2005, 5950, 185.		0
78	Supercontinuum generation in untapered and tapered photonic crystal fibers with two zero dispersion wavelengths. , 2005, 5733, 190.		0
79	The role of the second zero-dispersion wavelength in generation of supercontinua and bright-bright soliton-pairs across the zero-dispersion wavelength. Optics Express, 2005, 13, 6181.	3.4	196
80	Supercontinuum generation in a photonic crystal fiber with two zero-dispersion wavelengths tapered to normal dispersion at all wavelengths. Optics Express, 2005, 13, 7535.	3.4	132
81	Demonstration of the true-reflection OCT imaging algorithm on a heterogeneous multilayered structure. , 2004, , .		0
82	Monte Carlo modeling of optical coherence tomography systems. , 2004, , .		1
83	Advanced modelling of optical coherence tomography systems. Physics in Medicine and Biology, 2004, 49, 1307-1327.	3.0	35
84	Determination of optical scattering properties of highly-scattering media in optical coherence tomography images. Optics Express, 2004, 12, 249.	3.4	193
85	Extraction of optical scattering parameters and attenuation compensation in optical coherence tomography images of multilayered tissue structures. Optics Letters, 2004, 29, 1641.	3.3	55
86	Assessing blood vessel abnormality via extracting scattering coefficients from OCT images. , 2003, 5140, 12.		5